



CALPHAD-Type Assessment of the Pb-Se-Sn System

Ondrej Zobac¹ · Adela Zemanova¹ · Sinn-Wen Chen^{2,3} · Ales Kroupa¹

Submitted: 25 January 2022 / in revised form: 27 March 2022 / Accepted: 31 March 2022 / Published online: 11 May 2022
© ASM International 2022

Abstract CALPHAD-type theoretical assessment of the Pb-Se-Sn system was carried out. This assessment is part of a larger project aimed at developing an Ag-Pb-Se-Sn-Te thermodynamic database which should serve for the development of materials for thermoelectric applications. The experimental results from the literature were used but they are quite sparse and significant inconsistencies have been found between experimental data published by various authors, especially in the Se-rich regions. In general, a reasonable agreement was obtained for the theoretical and experimental sections of the phase diagram and for the enthalpies of mixing of the liquid phase in the region with low selenium content, but the agreement is rather qualitative in the Se-rich region.

Keywords CALPHAD · critical reassessment · Pb-Se-Sn phase diagram · ternary liquid phase

1 Introduction and Literature Review

Phase diagrams of thermodynamic systems are a crucial tool for the description as well as understanding of behavior and properties of both simple and

multicomponent systems. As such they are important for the development of new advanced materials and possible prediction of their materials properties. Detailed knowledge about the coexistence and stability of phases in stable or metastable equilibrium significantly rationalizes the design and preparation of complex materials with desired properties. Because experimental studies of multicomponent phase diagrams are very time consuming, and the extent of experimental work can be overwhelming, theoretical modelling of multicomponent phase diagrams is a very useful tool for materials development.

Interest in Se-based alloys has recently been renewed due to their possible importance in thermoelectric applications.^[1–5] The Pb-Se-Sn ternary system has been studied since the 1960s but there are still significant discrepancies in the results from different authors. A more detailed literature review is given below.

Wolley and Berolo^[6] proposed a pseudobinary section PbSe-SeSn in their paper based on x-ray powder analysis. Strauss^[7] experimentally studied the PbSe-SeSn section in the higher temperature range 700–1100 °C by thermal analysis and directly from as-cast samples (directly frozen ingots). Dal Corso et al.^[8] pointed to inconsistencies in previous works and published vertical sections PbSe-SnSe and PbSe-SnSe₂ respectively in the whole temperature range based on a combination of previous experimental results from thermal analysis (DTA, DSC), microstructural observations and their own experimental results. They proposed stabilization of the phase SeSn- β (high-temperature polymorph of SnSe intermetallic phase) to a lower temperature (approx. 425 °C) in the presence of lead and suggested significant solubilities of third elements in both PbSe and the SnSe family of intermetallic phases.

The experimental Pb-Se-Sn phase diagram has been published recently by Chen et al.,^[3] namely isothermal

✉ Ondrej Zobac
zobac@ipm.cz

¹ Institute of Physics of Materials, Czech Academy of Sciences, Zizkova 22, Brno, Czech Republic

² Department of Chemical Engineering, National Tsing Hua University, Hsinchu 300, Taiwan

³ High Entropy Materials Center, National Tsing Hua University, Hsinchu 300, Taiwan

sections for 350 and 500 °C. They did not observe any ternary phase in this system. The huge solubility of the third element was also observed in this work in the binary intermetallic phases PbSe and SeSn at the temperatures 350 and 500 °C in agreement with the work of Dal Corso et al.^[8] Chen et al.^[3] identified one polymorph of the binary intermetallic phase SeSn at both studied temperatures, probably low temperature SeSn- α . Nevertheless, this finding does not contradict the previous result of Dal Corso et al.^[8] Only two samples have been studied in the region where the phase change should appear, and it is not easy to distinguish between the two phases.

Partial liquidus surface was studied by Zlomanov et al.^[9] and the liquidus surface in the whole concentration range was presented by Saveliev et al.^[10] Experimentally measured enthalpies of mixing in liquid at 763, 845 and 970 °C were published by Kotchi et al.^[11]

An attempt to theoretically model a part of the Pb-Se-Sn phase diagram was made by Laugier et al.^[12] who applied a regular associated solution model to calculate the T-x ternary liquid-solid phase equilibrium of the PbSe-SnSe section of the phase diagram and the liquid surface of the Pb-Se-Sn system. Good agreement with experiments was obtained for the liquid-solid equilibrium between liquid and PbSe intermetallic phase with rocksalt structure. Full thermodynamic CALPHAD-based assessment of the ternary phase diagram has not yet been published up to now.

The phases existing in the Pb-Se-Sn system together with their crystallographic structures are listed in the Table 1.

2 Thermodynamic Modelling

The CALPHAD approach^[14,15] was used for thermodynamic modelling and calculation of phase diagrams. The compositions of phases in equilibrium correspond to the minimum total Gibbs energy of a closed system at constant temperature and pressure. Calculations were performed

using Thermo-Calc^[16] and Pandat^[17] software, which solve the constrained minimization problem to determine the set of non-negative number of individual components in equilibrium phases. The Gibbs energies are considered relative to the Standard Element Reference state (SER). The Gibbs energy data for pure elements were taken from the SGTE database for pure elements ver. 5.0.^[18]

2.1 The Solution Phases

The Gibbs energies of terminal solid solutions were mostly modelled using a substitutional model with one sublattice.

The substitutional solution model with associates was used for the thermodynamic description of the molar Gibbs energy of the liquid phase. It assumes mutual mixing of three elements Pb, Se, Sn and two associates PbSe and SeSn (in agreement with the models for liquid in the respective binary subsystems)

The molar Gibbs energy of the solution phase α is expressed as:

$$G_m^\alpha(T, x^\alpha) = {}^0 G_m^\alpha(T) + {}^{id} G_m^\alpha(T, x^\alpha) + {}^E G_m^\alpha(T, x^\alpha) \quad (\text{Eq 1})$$

where the first term is the molar reference Gibbs energy, which is the weighted sum of the Gibbs energies of the system constituents i in the crystallographic structure of the phase α or in the liquid state relative to the selected reference state.

The second term of Eq 1 is the contribution to the total Gibbs energy resulting from the ideal mixing of the constituents in the crystal lattice of the phase α or in the liquid, where n is the number of constituents Eq 2.

$${}^{id} G_m^\alpha = RT \sum_{i=1}^n x_i \cdot \ln(x_i) \quad (\text{Eq 2})$$

Third term, the excess Gibbs energy ${}^E G_m^\alpha$, describes the influence of the non-ideal behaviour of the system on the thermodynamic properties of the phase and is given by the Redlich-Kister-Muggianu formalism.^[19,20]

Table 1 The crystallographic structure of phases existing in the system

Common phase name	Phase name in database	Pearson symbol	Structure type	Ref.
(Pb)	FCC_A1	cF4	Pb	Ref 22
(Se)	HEX_A8	hP3	Se	Ref 13
(β Sn)	BCT_A5	tI4	β Sn	Ref 13
(α Sn)	DIAMOND_A4	cF8	C(diamond)	Ref 13
PbSe	PBSE	cF8	NaCl	Ref 22
Se ₂ Sn	SE2SN	hP3	CdI ₂	Ref 13
SeSn- α	SESN_ALPHA	oP8	GeS	Ref 13
SeSn- β	SESN_BETA	oC8	CrB	Ref 13

$$E G_m^\alpha = \sum_{\substack{i,j=1 \\ i \neq j}}^n x_i x_j \sum_{z=0}^m z L_{i,j}(x_i - x_j) + \sum_1^{n-2} \sum_{j=i+1}^{n-1} \sum_{k=j+1}^n x_i \cdot x_j \cdot x_k \cdot L_{i,j,k} \tag{Eq 3}$$

where $zL_{i,j}$ are the temperature dependent binary interaction parameters describing the mutual interaction between constituent i and j , and $L_{i,j,k}$ is the interaction parameter describing the possible ternary interactions. Their temperature dependence is usually defined as:

$$L(T) = a + bT + cT \ln(T) \tag{Eq 4}$$

The substitutional solid solution phases of the elements β -Sn (bct_A5), α -Sn (diamond_A4) and Se (hexagonal_A8) were modelled by solid solution model described above. With respect to very low solubilities of other elements (especially Se) in the terminal solid solutions, the substitutional solid solution model for (β -Sn) was defined as (PB, SN)1 and no solubility of other elements were assumed for (α -Sn) and (Se).

The substitutional model with associates for liquid used in the database is labelled LIQUID and defined as (PB, PBSE, SE, SN, SNSE)1.

The Pb (fcc_A1) terminal solid solution was modelled by two-sublattice interstitial solid solution model. This model assumed that the metallic elements could substitute each other in the metal sublattice, and interstitial elements and vacancies exist in the interstitial sublattice. Because there are no interstitial elements in this system, the model corresponds from the practical point of view to the above shown substitutional model, nevertheless this model is selected to be consistent with other databases containing the fcc_A1 phase. The specific model for the solid solution fcc_A1 (Pb) in the database was therefore named FCC_A1 and defined as (PB,SN)1(VA)1.

2.2 Intermetallic Phases

The Pb-Se-Sn ternary system contains 4 intermetallic phases (PbSe, SeSn- α , SeSn- β , Se2Sn), which are stoichiometric in binary systems but exhibit the solubility of the third element in their structures in the ternary system. The Compound Energy Formalism is used to model intermetallic phases. Basic principles for the case of two sublattices are shown here, as two-sublattice models were used in this assessment. Details of this approach can be found e.g. in Ref 14,15

In the case of the PbSe phase each sublattice is occupied by one basic element and Sn substitutes Pb in the relevant

sublattice ((PB, SN)1(SE)1). The name of the phase is PBSE in the database. Similarly, Pb substitutes Sn in the SeSn family of phases and the Se2Sn phase ((SE)0.5(PB, SN)0.5 and (SE)0.66667(PB, SN)0.33333, respectively). The names of the phases are SESN_ALPHA, SESN_BETA and SE2SN in the database.

The reference Gibbs energy corresponding to the Eq 1 for constituents i and j is given as:

$$G_{ref}^\alpha = \sum y_i \cdot y_j \cdot G_{(ij)} \tag{Eq 5}$$

where the y_i terms are the site fractions of each constituent in the sublattice 1 or 2. The term $G(i;j)$ describes the Gibbs energy of formation of the so-called “end member” ij .

The ideal mixing term is given by

$$G_{id}^\alpha = \sum_{p=1}^2 f_p \cdot \sum_{i=1}^n p y_i \cdot \ln(p y_i) \tag{Eq 6}$$

where f_p is the stoichiometric coefficient for a sublattice p and the second sum describes the effect of the ideal mixing within the sublattice p . The contribution of the excess Gibbs energy for the two-sublattice model with three constituents i, j, k is defined as:

$$G_E^\alpha = \sum y_i \cdot y_j \cdot y_k L_{(i,j,k)} + \sum y_i \cdot y_k \cdot y_l L_{(i,k,l)} \tag{Eq 7}$$

where

$$L_{(i,j,k)} = \sum_z z L_{(i,j,k)} \cdot (y_i - y_j)^z \tag{Eq 8}$$

The parameters $zL_{i,j;k}$ describe the mutual interaction of constituents i and j in the first sublattice when the second sublattice is fully occupied by constituent k . This description can be extended to any number of sublattices.

The individual models of intermetallic phases are listed in the Table 2. The two-sublattice model is used for all phases.

2.3 Binary Systems

Binary data of constituting subsystems are necessary for modelling the ternary system and they are used for ternary extrapolation of the Pb-Se-Sn system. The prediction provides us with basic knowledge about the phase equilibria in the system but cannot provide information about the solubility of the third element in the binary phases or the existence of a possible ternary phase. Thermodynamic descriptions of binary subsystems are known and accepted from the literature.

Se-Sn binary phase diagram was published by Feute-lais et al.^[21] It contains a family of intermetallic phases

Table 2 Thermodynamic parameters for optimized phases in the Pb-Se-Sn ternary system and binary subsystems

Phase name (Sublattice model)	Parameter	Value	Ref.	
LIQUID (PB,PBSE,SE,SESN,SN)	${}^0G_{PbSe}^{LIQ}$	$- 91032.45 + 29.88*T + G_{Pb}^{LIQ} + G_{Se}^{LIQ}$	Ref 22	
	${}^0G_{SnSe}^{LIQ}$	$- 134591.86 + 278.59972*T - 32.99*T*\ln(T) + G_{Pb}^{LIQ} + G_{Se}^{LIQ}$	Ref 21	
	${}^0L_{Pb,Sn}^{LIQ}$	$+6204.5 - 0.67981*T$	Ref 23	
	${}^1L_{Pb,Sn}^{LIQ}$	$+ 791.7 - 1.5219*T$	Ref 23	
	${}^0L_{Pb,PbSe}^{LIQ}$	$+ 19500.32$	Ref 22	
	${}^1L_{Pb,PbSe}^{LIQ}$	$- 1003.26 + 0.58*T$	Ref 22	
	${}^2L_{Pb,PbSe}^{LIQ}$	$+ 8352.21 - 5.64*T$	Ref 22	
	${}^0L_{PbSe,Se}^{LIQ}$	$+ 17503.24 - 7.95*T$	Ref 22	
	${}^1L_{PbSe,Se}^{LIQ}$	$+ 4201.24 - 6.42*T$	*	
	${}^2L_{PbSe,Se}^{LIQ}$	$+ 16498.24 - 3.61*T$	Ref 22	
	${}^0L_{Se,SnSe}^{LIQ}$	$+ 15432.8 - 19.06391*T$	Ref 22	
	${}^1L_{Se,SnSe}^{LIQ}$	$+8995.55$	Ref 21	
	${}^0L_{Sn,SnSe}^{LIQ}$	$+ 43462.43 - 21.6074*T$	Ref 21	
	${}^1L_{Sn,SnSe}^{LIQ}$	$- 1032.5$	Ref 21	
	${}^0L_{PbSe,Se,SnSe}^{LIQ}$	$+ 1.916923E + 05 - 307.69*T$	*	
	${}^1L_{PbSe,Se,SnSe}^{LIQ}$	$-1.079120E+06+420.5*T$	*	
	${}^2L_{PbSe,Se,SnSe}^{LIQ}$	$- 3.032750E + 05 + 175*T$	*	
	${}^0L_{Pb,PbSe,SnSe}^{LIQ}$	$- 80000$	*	
	${}^1L_{Pb,PbSe,SnSe}^{LIQ}$	$- 80000 - 30*T$	*	
	${}^2L_{Pb,PbSe,SnSe}^{LIQ}$	0	*	
	${}^0L_{PbSe,SnSe}^{LIQ}$	$-0.208615E + 04 - 33.8461*T$	*	
	${}^1L_{PbSe,SnSe}^{LIQ}$	$- 30.584615E + 03 + 15.3846*T$	*	
	${}^2L_{PbSe,SnSe}^{LIQ}$	$+ 1.041846E + 04 - 21.5385*T$	*	
	${}^0L_{Pb,SnSe}^{LIQ}$	$- 1207.69 - 7.692*T$	*	
	${}^1L_{Pb,SnSe}^{LIQ}$	0	*	
	${}^2L_{Pb,SnSe}^{LIQ}$	0	*	
	BCT_A5 (Sn-β) (PB,SN)	${}^0L_{Pb,Sn}^{BCT_A}$	$+ 19700 - 15.89*T$	Ref 23
	DIAMOND_A4(Sn-α) (SN) ₁	$G_{Sn}^{DIA_A4}$	$G_{Sn}^{DIA_A4}$	Ref 18
FCC_A1 (Pb) (PB,SN) ₁ (VA) ₁	${}^0L_{Pb,Sn:Va}^{FCC_A1}$	$+ 7145.3 - 2.30237*T$	Ref 23	
HEX_A8 (Se) (SE) ₁	$G_{Se}^{HEX_A8}$	$G_{Se}^{HEX_A8}$	Ref 18	
PBSE (PbSe) (PB,SN) ₁ (SE) ₁	${}^0G_{Pb:Se}^{PbSe}$	$- 99783.25 + 22.52*T + G_{Pb}^{HSER} + G_{Se}^{HSER}$	*	
	${}^0G_{Sn:Se}^{PbSe}$	$+ 5000 + G_{Sn}^{HSER} + G_{Se}^{HSER}$	*	
	${}^0L_{Pb,Sn:Se}^{PbSe}$	$- 3.125758E + 05 + 68.34*T$	*	
	${}^1L_{Pb,Sn:Se}^{PbSe}$	$- 92000 + 92*T$	*	
	${}^2L_{Pb,Sn:Se}^{PbSe}$	$- 10000 + 15*T$	*	
SE2SN (Se ₂ Sn) (SE) _{0.66667} (PB,SN) _{0.33333}	${}^0G_{Se:Sn}^{Se2Sn}$	$- 46104.05 + 121.16205*T$ $- 24.84*T*\ln(T) - 0.00164*T^2 + 39347*T^{-1} + 1.185733E - 07*T^3$	Ref 21	
	${}^0G_{Se:Pb}^{Se2Sn}$	$0.66667* G_{Se}^{HSER} + 0.33333* G_{Pb}^{HSER} + 15000$	*	
	${}^0G_{Se:Pb,Sn}^{Se2Sn}$	$- 60000$	*	
SESN_ALPHA (SeSn-α) (SE) _{0.5} (PB,SN) _{0.5}	${}^0G_{Se:Sn}^{SeSn_alpha}$	$- 63171.87 + 134.4964*T - 26.31*T*\ln(T) - .00182* T^2 + 61422.5* T^{-1} + 1.1076E - 07* T^3$	Ref 21	
	${}^0G_{Se:Pb}^{SeSn_alpha}$	$+ 15000 + 0.5*G_{Se}^{HSER} + 0.5*G_{Pb}^{HSER}$	*	
	${}^0L_{Se:Pb,Sn}^{SeSn_alpha}$	$-171000+65*T$	*	
	${}^1L_{Se:Pb,Sn}^{SeSn_alpha}$	$- 40000 - 10*T$	*	
	${}^2L_{Se:Pb,Sn}^{SeSn_alpha}$	$-88850+50*T$	*	
SESN_BETA (SeSn-β) (SE) _{0.5} (PB,SN) _{0.5}	${}^0G_{Se:Sn}^{SeSn_beta}$	$- 62529.58 + 133.69002*T - 26.31*T*\ln(T) - .00182* T^2 + 61422.5* T^{-1} + 1.1076E - 07* T^3$	Ref 21	
	${}^0G_{Se:Pb}^{SeSn_beta}$	$+ 15000 + 0.5*G_{Se}^{HSER} + 0.5*G_{Pb}^{HSER}$	*	
	${}^0L_{Se:Pb,Sn}^{SeSn_beta}$	$-171284 + 65*T$	*	

Table 2 continued

Phase name (Sublattice model)	Parameter	Value	Ref.
	${}^1L_{\text{SeSn}_\beta\text{beta}_{\text{Se:Pb,Sn}}}$	$-40000 - 9.8 * T$	*
	${}^2L_{\text{SeSn}_\beta\text{beta}_{\text{Se:Pb,Sn}}}$	$-88850 + 50 * T$	*

Unary data are from SGTE database^[18]

*Parameter assessed in this work

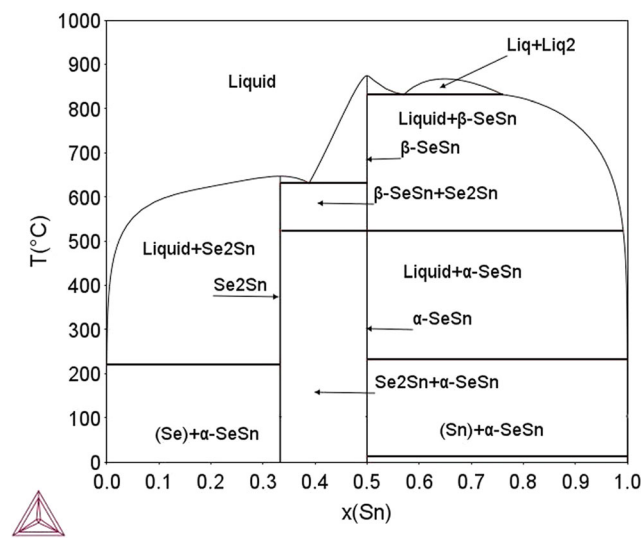


Fig. 1 The Se-Sn phase diagram calculated using the data of Feutalais et al.^[21]

SeSn, low-temperature SeSn- α and high-temperature SeSn- β modification. There is also Se2Sn intermetallic phase in the system. All three phases are modelled as stoichiometric. The liquid phase contains the SNSE associate. In the Sn-rich region, there is a small miscibility gap in liquid.

Thermodynamic assessment of the Pb-Se system was published by Liu et al.^[22] The assessment was slightly modified in the scope of this work, as there was a slight disagreement between the invariant temperature for the $L1 \rightarrow PbSe + L2$ published in Ref 22 and obtained by calculation using original dataset from the same work. The reason for this discrepancy might be caused by a typographical error. There is one intermetallic phase PbSe in the system and the liquid phase model includes the PBSE associate. The Pb-Se phase diagram also exhibits a liquid miscibility gap in the Se-rich region.

ALPHAD modelling of the Pb-Sn binary subsystem is adopted from Ohtani et al.^[23] This phase diagram is of simple eutectic type.

The calculated phase diagrams of the binary subsystems are shown in Fig. 1, 2 and 3. The thermodynamic parameters and models of the existing phases for all binary subsystems are summarized in Table 2.

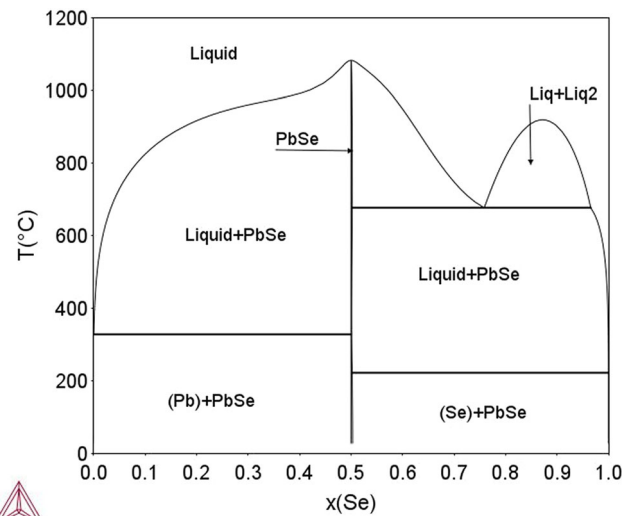


Fig. 2 The Pb-Se phase diagram calculated using the data of Liu et al.^[22]

3 Theoretical Results

The thermodynamic assessment of the ternary system was carried out using the Thermo-Calc and Pandat software packages. The above-mentioned binary assessments were used together with the experimental phase data from Ref 3,8 and 10. Experimentally measured enthalpies of mixing of liquid presented in Ref 11 were also used. As already mentioned in the Introduction, there are significant inconsistencies between the experimental data, and therefore not all data in the literature were accepted in the assessment. A more detailed discussion can be found in the relevant part of Sect. 4 (Discussion). The thermodynamic parameters for the ternary system assessed in this work and the parameters for the binary subsystems are listed in Table 2.

Two isothermal sections at 350 and 500 °C were presented in Ref 3 and a quasi-binary PbSe-SnSe section was established in Ref 8. The PbSe-Se2Sn vertical section was also studied in Ref 8 however, there is very strong inconsistency between the phase equilibria in this vertical section and the relevant phase equilibria in the isothermal sections from Ref 3. The results from Ref 3 were used for the assessment because there is a good consistency between the two experimental isothermal sections and the results obtained after long-term annealing are supported by

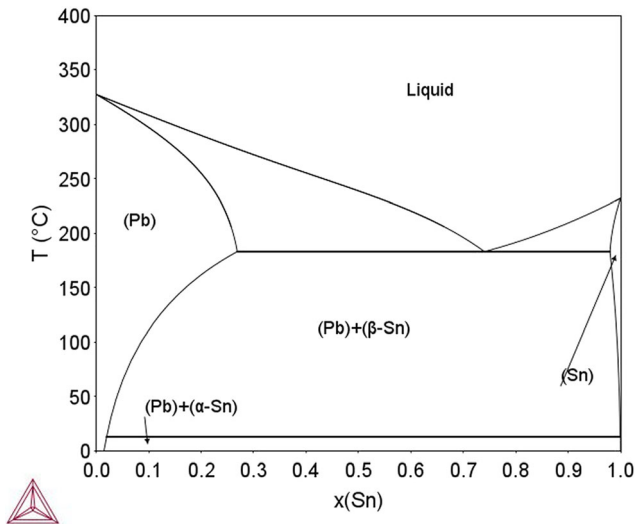


Fig. 3 The Pb-Sn phase diagram calculated using the data from Ohtani et al.^[23]

micrographs, x-ray analysis and EDX composition measurements. The quasi-binary section from Ref 8 was also used as it is consistent with results from Strauss^[7]. These sections of phase diagrams are shown in Fig. 4, 5 and 6.

In the following text, the Se-rich liquid phase is referred to as Liquid(Se), the (Pb,Sn)-rich liquid is designated as Liquid(Pb), and the liquid phase with content of about 10 at.% Pb and 10–20 at.% Sn is labelled as Liquid(ter).

The thermodynamic properties of the Pb-Se-Sn system were studied in Ref 11. The authors measured the enthalpies of mixing of liquid in the system at 763, 845 and 970 °C for different x_{Pb}/x_{Sn} and x_{Se}/x_{Pb} ratios. Unfortunately, they did not publish all the obtained experimental data, they only presented the results for selected sections with different concentration ratios and temperatures in the form of tables and figures. The comparison of the experimental results with the calculated enthalpies of mixing was performed for characteristic sections and the results are presented in Fig. 7, 8, 9, 10, 11, 12, 13 and 14.

The complete liquidus surface of the Pb-Se-Sn system was presented in Ref 10. Unfortunately, this paper is very concise, and no details are published in the paper. The authors did not provide any information on the experimental condition other than that the DTA method was used. No sample compositions and other necessary data are available. On the other hand, the liquidus surface looks reasonable for most of the concentration regions. The calculated and experimentally established liquidus surfaces are shown in Fig. 15(a), (b) and (c).

Invariant reactions containing liquid phases existing in the Pb-Se-Sn system are listed in the Table 3.

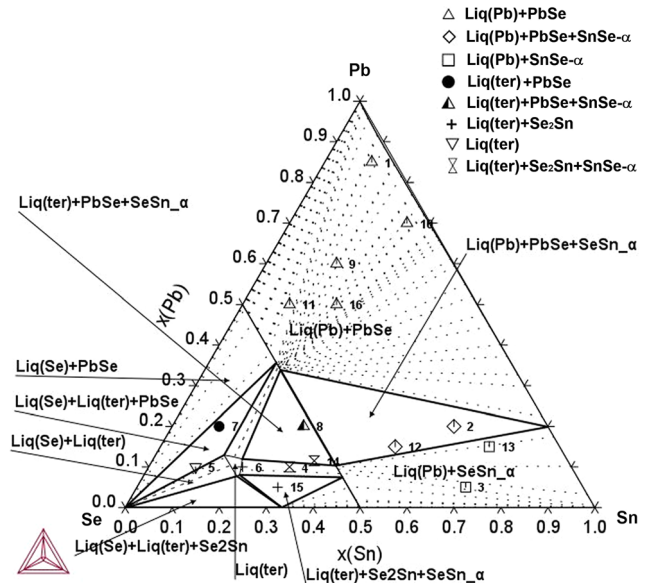


Fig. 4 Isothermal section of phase diagram Pb-Se-Sn at 350 °C with superimposed experimental data from Ref 3. The legend describes experimental equilibria. The numbers of samples correspond to the samples listed in Table 1 in Ref 3.

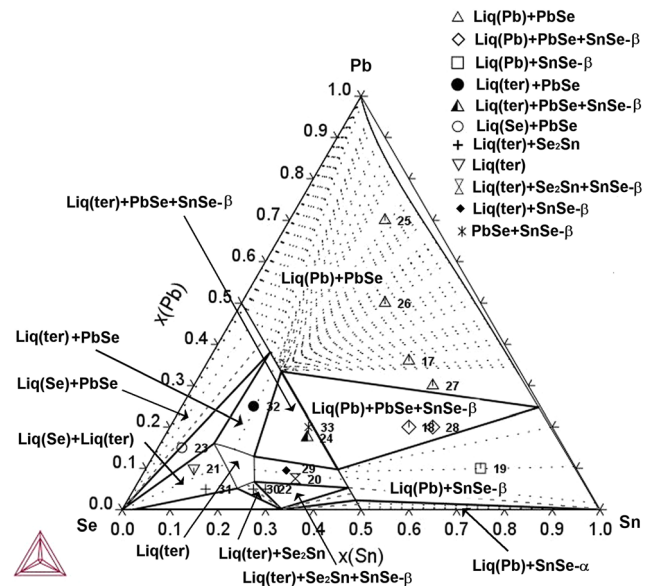


Fig. 5 Isothermal section of phase diagram Pb-Se-Sn at 500 °C with superimposed experimental data from Ref 3. The legend describes experimental equilibria. The numbers of samples correspond to the samples listed in Table 3 in Ref 3.

4 Discussion

The analysis of present results and their comparison with experiments shows only an average agreement for some calculations. One of the main reasons for the worse agreement is the inconsistency of experimental results from

Fig. 6 Pseudobinary vertical section between PbSe and SnSe. The experimental data from DTA measurements are from Ref 8

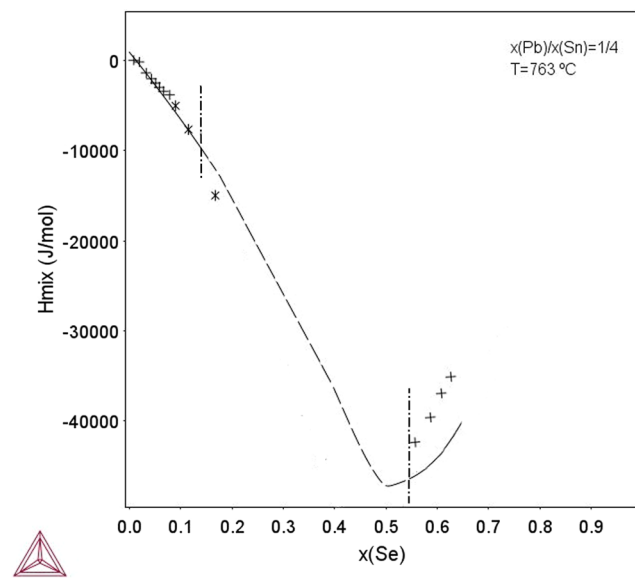
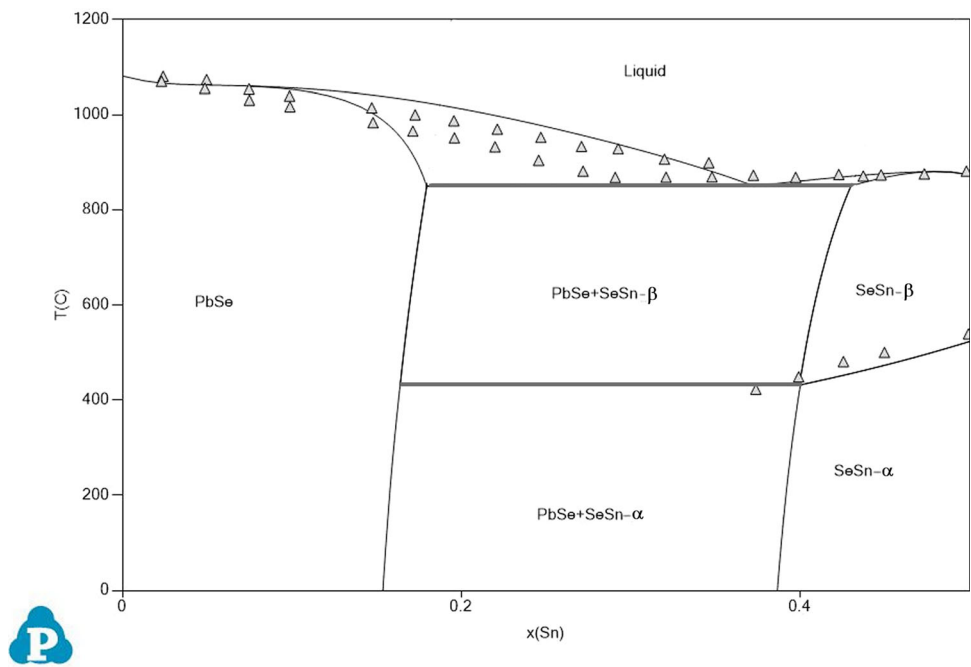


Fig. 7 Calculated enthalpy of mixing of liquid for the ratio Pb/Sn=1/4 at the temperature 763 °C in comparison with experimental data from Ref 11. Dot-dashed lines indicate the extent of pure liquid phase obtained from calculation., + indicates experimental data for single phase liquid and * indicates data for a two-phase mixture with liquid.^[11] Pure liquid elements at the temperature of measurements are selected as reference states

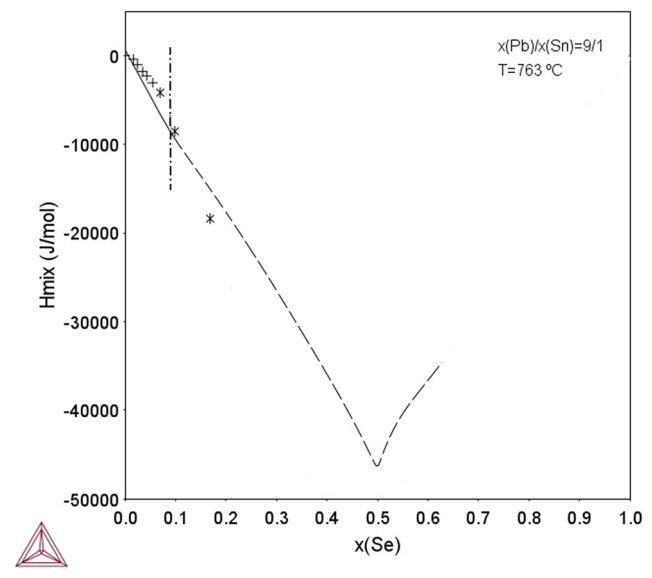


Fig. 8 Calculated enthalpy of mixing of liquid for the ratio Pb/Sn=9/1 at the temperature 763 °C in comparison with experimental data from in Ref 11. Dot-dashed line indicate the extent of pure liquid phase obtained from calculation., + indicates experimental data for single phase liquid and * indicates data for a two-phase mixture with liquid.^[11] Pure liquid elements at the temperature of measurements are selected as reference states

different authors. In general, the agreement is worse for Se-rich regions both for the phase diagram sections and the thermodynamic measurements.

The calculated isothermal sections at 350 and 500 °C from Ref 3 show a very good agreement for the region with less than 50 at.% Se. Here, all experimental results agree well with the calculated phase equilibria. There is only a

qualitative agreement in the Se-rich corner, all experimentally found phase fields are correctly modelled, but the discrepancy is in the positions of specific phase fields especially in 350 °C isothermal section.

The key discrepancy exists in the shape and size of the pure liquid region, which exists around 10 at.% Pb and 10-20 at.% Sn. Two variants for the extent and position of

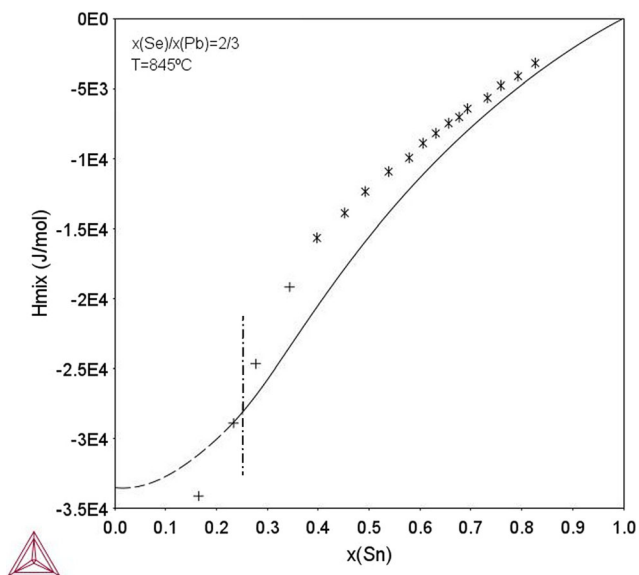


Fig. 9 Calculated enthalpy of mixing of liquid for the ratio Se/Pb=2/3 at the temperature 845 °C in comparison with experimental data from Ref 11. Dot-dashed line indicate the extent of pure liquid phase obtained from calculation., + indicates experimental data for single phase liquid and * indicates data for a two-phase mixture with liquid.^[11] Pure liquid elements at the temperature of measurements are selected as reference states

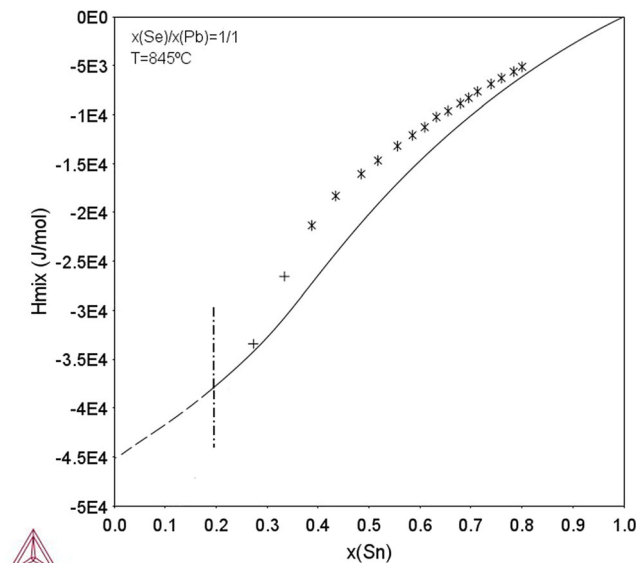


Fig. 10 Calculated enthalpy of mixing of liquid for the ratio Se/Pb=1/1 at the temperature 845 °C in comparison with experimental data from Ref 11. Dot-dashed line indicate the extent of pure liquid phase obtained from calculation., + indicates experimental data for single phase liquid and * indicates data for a two-phase mixture with liquid.^[11] Pure liquid elements at the temperature of measurements are selected as reference states.

this phase field were proposed in the work,^[3] one where a very narrow phase field connected with the pure liquid selenium exists (Fig. 1(b) in Ref 3) and second where a

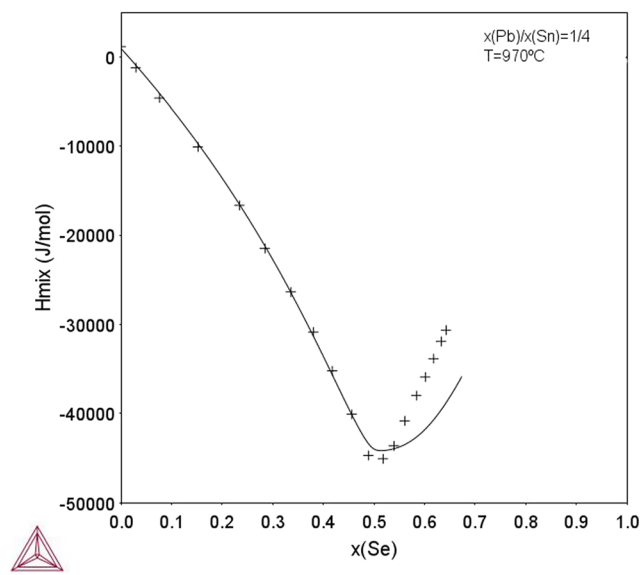


Fig. 11 Calculated enthalpy of mixing of liquid for the ratio Pb/Sn=1/4 at the temperature 970 °C; + indicates the experimental results from Ref 11. Pure liquid elements at the temperature of measurements are selected as reference states.

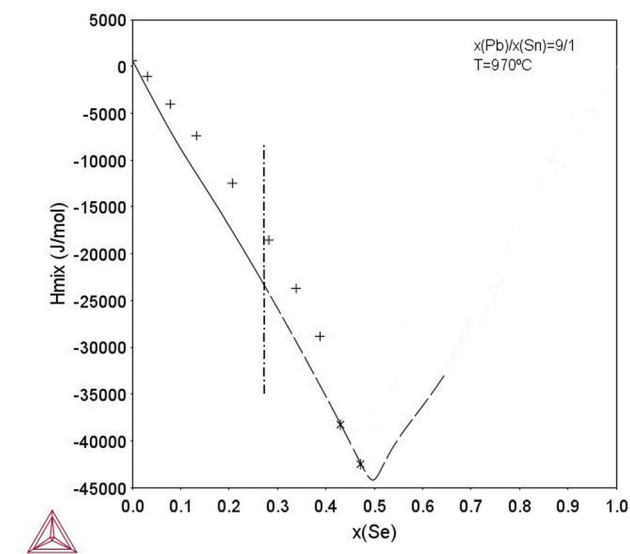


Fig. 12 Calculated enthalpy of mixing of liquid for the ratio Pb/Sn=9/1 at the temperature 970 °C in comparison with experimental data from Ref 11. Dot-dashed line indicate the extent of pure liquid phase obtained from calculation., + indicates experimental data for single phase liquid and * indicates data for a two-phase mixture with liquid.^[11] Pure liquid elements at the temperature of measurements are selected as reference states.

separate liquid phase field connected with the Se-rich liquid by two-phase field labelled (Liquid(Se) + Liquid(ter)) as shown in Fig. 1(c) in Ref 3. The selection of a more likely phase equilibrium was not done due to the lack of experimental samples in that region. Theoretical modelling strongly supported the existence of the two-phase field

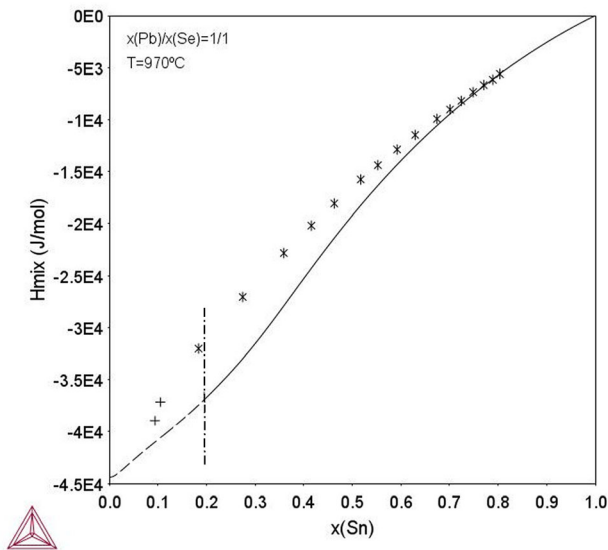


Fig. 13 Calculated enthalpy of mixing of liquid for the ratio Pb/Se=1/1 at the temperature 970 °C in comparison with experimental data from Ref 11. Dot-dashed line indicate the extent of pure liquid phase obtained from calculation., + indicates experimental data for single phase liquid and * indicates data for a two-phase mixture with liquid^[11]. Pure liquid elements at the temperature of measurements are selected as reference states

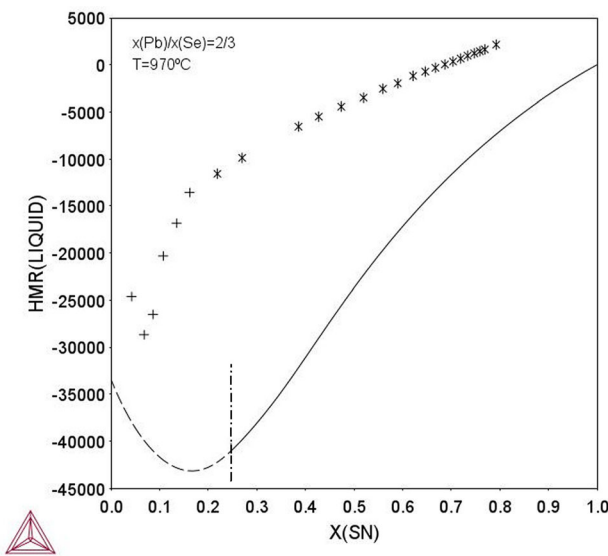


Fig. 14 Calculated enthalpy of mixing of liquid for the ratio Pb/Se=2/3 at the temperature 970 °C in comparison with experimental data from Ref 11. Dot-dashed line indicate the extent of pure liquid phase obtained from calculation., + indicates experimental data for single phase liquid and * indicates data for a two-phase mixture with liquid^[11]. Pure liquid elements at the temperature of measurements are selected as reference states

(Liquid(Se) + Liquid(ter)), nevertheless, the extent of the experimentally found Liquid(ter) phase field does not correspond to the calculated one. The calculated one is

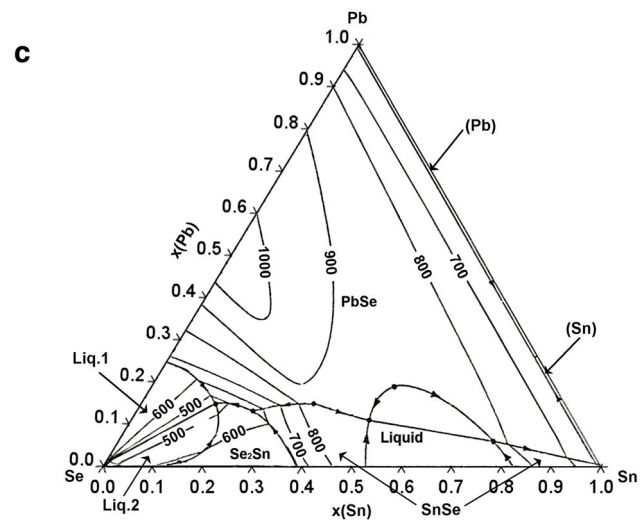
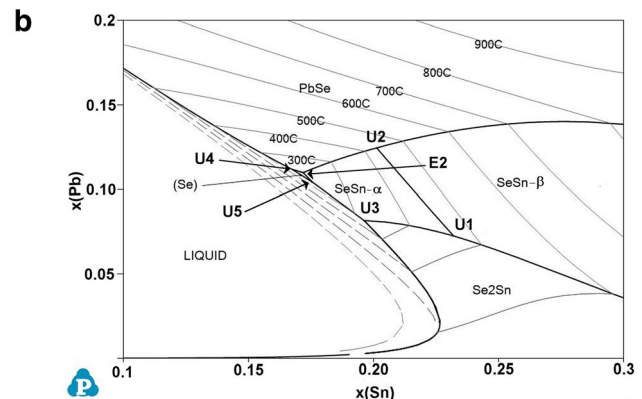
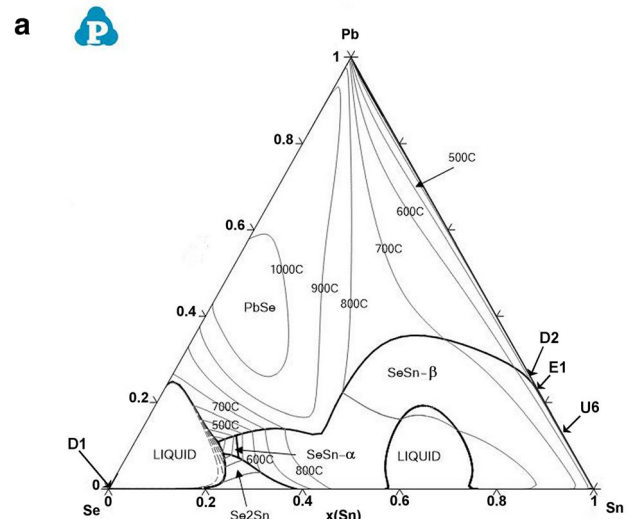


Fig. 15 (a) Calculated liquidus surface of Pb-Se-Sn phase diagram, (b) detail of the liquidus surface in the Se-rich corner, (c) the experimentally established liquidus surface from Ref 10

significantly smaller and shifted slightly towards a higher Sn content. It has been found that any attempt to model a

Table 3 The calculated invariant reactions containing liquid phases in the system Pb–Se–Sn

Type of reaction	<i>T</i> (°C)	Invariant reaction	Overall composition		
			<i>x</i> (Pb)	<i>x</i> (Se)	<i>x</i> (Sn)
U1	465.4	SeSn-β + Se ₂ Sn => Liq + SeSn-α	0.072	0.696	0.232
U2	431.9	Liq + SeSn-β => PbSe + SeSn-α	0.125	0.674	0.201
E1	431.9	SeSn-β => Liq. + PbSe + SeSn-α	0.223	0.001	0.775
U3	315.8	Liq + Se ₂ Sn => SeSn-α + Liq	0.082	0.722	0.196
U4	220.8 ₄	Liq + PbSe => Liq + (Se)	0.112	0.721	0.167
U5	220.8 ₃	Liq + Liq => SeSn-α + (Se)	0.104	0.720	0.175
D1	220.7 ₇	Liq + SeSn-α => Se ₂ Sn +(Se)	0	0.999	0.001
E2	205.3	Liq => (Se) + PbSe + SeSn-α	0.110	0.718	0.172
U6	203.6	Liq + SeSn-α => PbSe +(Sn)	0.129	0	0.871
D2	183.0	Liq => (Pb)+PbSe+(Sn)	0.260	0	0.740

Italic values indicate the amount of this element in given IR is smaller than 0.001

larger phase field, especially extended in the direction of Sn axis, leads to an expansion of the liquid phase well below 200 °C and to the existence of a very complicated multiple liquid miscibility gap structure at high temperatures not only in the Se-rich region.

Thus, the agreement is only qualitative for the section at 350 °C, all experimentally determined phase fields are present in the calculated section, however, their shape and position are to some extent different.

Rather better agreement was obtained for the isothermal section for 500 °C. Here, too, the agreement is very good for the Se-poor region, with only one exception. The SnSe-β was not identified in Ref 3 They did not consider the HT modification, probably because the transition temperature for binary SnSe-α/β intermetallics is well above 500 °C. However, according to the work,^[8] the high solubility of Pb in the SnSe family of phases leads to the stabilization of the HT modification of the SnSe intermetallic phase in the low temperature region below 500 °C.

The concentration dependence of the α/β transition temperature was modelled with respect to the data^[8] and the phase boundaries are shown for the SnSe-α + SnSe-β + Liq(Pb) phase field in Fig. 5 (the liquid phase rich in Pb and/or Sn is labeled Liquid(Pb) in the text and figures in this paper). It can be seen from Fig. 5 that the samples were only available in the assumed SnSe-β + Liq(Pb) phase field.

Better agreement was obtained for the Se-rich region of the 500 °C section compared to the 350 °C section. Especially the samples 23 and 32 agree well with the experimental results and confirmed the existence of a liquid miscibility gap in this region. The sample 23 clearly showed the existence of (Liquid(Se) + PbSe), where the liquid phase contained almost 99 at.% of Se. Sample 32 consists of PbSe phase together with Liquid(ter) with a composition of Pb-64.4 at.% Se-19.4 at.%Sn.

The PbSe–SnSe-α/β quasi-binary section is shown in Fig. 6. Here, a reasonable agreement was obtained for the liquidus line and the concentration dependence of the SnSe-α/β transition temperature with the experimental results from Ref 8. The value of eutectic temperature also agreed well with the experiment. Nevertheless, there is a significant difference for the PbSe/(PbSe + Liq) phase boundary. Thermodynamic modelling predicts much lower solubility of Sn in the PbSe intermetallic phase especially around the eutectic temperature. The values of Sn solubility in PbSe at 350 and 500 °C were accepted from Ref 3 because no other data are available for such low temperatures. The attempt to model high Sn solubility in PbSe at high temperatures led to a very strong temperature dependence for the relevant interaction parameters and consequently it was not possible to model a reasonable liquidus surface for the ternary system. Pseudo-ternary (Pb,Sn)Se phase was stabilized by tin at very high temperatures above 1500 °C and as mentioned above, all attempts to model the correct liquidus surface and the correct stability of (Pb,Sn)Se led again to multiple miscibility gaps and very unlikely shape of the liquidus surface.

The enthalpies of mixing for the three temperatures and various Pb/Sn and Pb/Se ratios were measured by Ref 11. The experimental difficulties encountered in this system were demonstrated in the published results and it can be concluded that a higher amount of Se usually meant a greater discrepancy between experiments and modelling. Some of the presented experimental results are questionable, which is also demonstrated here.

Figure 7 and 8 show a comparison between two sections with *x*(Pb)/*x*(Sn)=1/4 and 9/1, respectively, for the temperature 763 °C. Here, a single liquid phase exists in two separate concentration intervals and good agreement was obtained only for a low concentration of Se in this limited interval. Experimental data for the liquid phase in the

concentration region of approx. $x(\text{Se}) = 0.55 - 0.7$ show worse agreement. Experimental data are not available for high selenium content (approx. $x(\text{Se}) > 0.7$), where the liquid miscibility gap exists. Experimental difficulties are probably the reason for the lack of data. Dot-dashed lines indicate the calculated position of the phase boundary between the liquid and the two-phase field. The experimentally established phase boundary is in the interval between two measurements labeled by symbols + (single phase liquid) and * (two-phase with liquid). The agreement is good considering the small amount of experimental data and the uncertainty of the experimental liquidus surface (to be discussed later). Dashed line shows the calculated values of the enthalpy of mixing of liquid in the metastable region.

Figures 9 and 10 show a comparison between experimental and calculated values for two sections with $x(\text{Se})/x(\text{Pb}) = 2/3$ and $1/1$, respectively, at the temperature $845\text{ }^\circ\text{C}$. Here the tendency is well reproduced by calculations, but the differences between the experimentally and theoretically determined boundaries of the liquid phase field are worse.

The experimental results at $970\text{ }^\circ\text{C}$ were presented for several sections both for Se/Pb and Pb/Sn ratios in.^[11] The results for the $x(\text{Pb})/x(\text{Sn}) = 1/4$ and $9/1$, respectively, are shown in Fig. 11 and 12. Only a liquid phase exists for the first ratio at this temperature and the excellent agreement of the measured and calculated enthalpies of mixing was obtained for $x(\text{Se}) < 0.5$. There is also a very good agreement for the limiting enthalpy of mixing in the binary

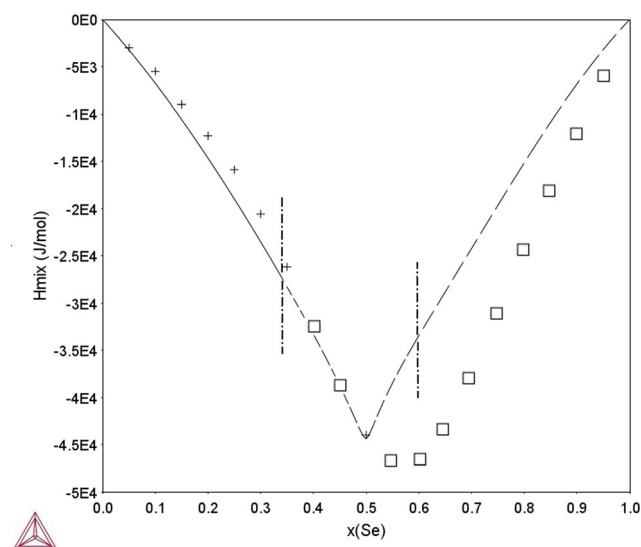


Fig. 16 Calculated enthalpy of mixing of liquid for the binary Pb-Se system at the temperature $970\text{ }^\circ\text{C}$ in comparison with experimental data from Ref 11. The dashed line marked two phase region, □—extrapolated values from Ref 11. Pure liquid elements at the temperature of measurements are selected as reference states.

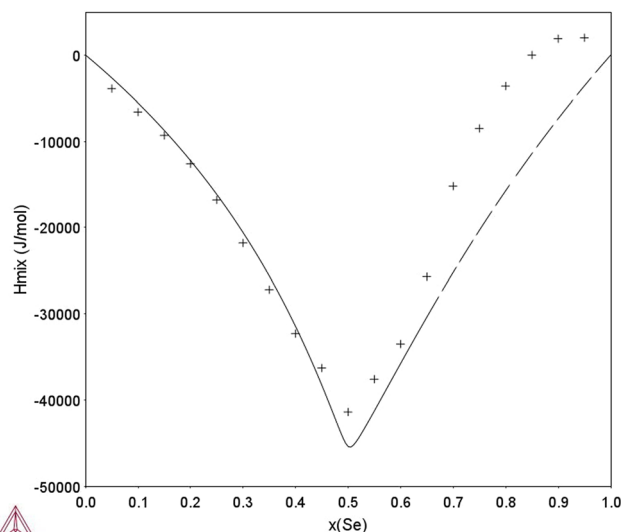


Fig. 17 Calculated enthalpy of mixing of liquid for the binary Se-Sn system at the temperature $970\text{ }^\circ\text{C}$ in comparison with experimental data from Ref 11. Pure liquid elements at the temperature of measurements are selected as reference states

Pb-Sn system. The experimental data are only available for $x(\text{Se}) < 0.643$, but in the Se-rich region, the agreement is significantly worse. A slightly worse agreement was obtained for the second ratio, but the tendency is still well reproduced. This discrepancy can be caused by significant problems in measuring the respective enthalpies of mixing in liquid for samples with a high selenium content. Such problems also occur in binary systems, where there are significant differences between the experimental enthalpies of mixing of liquid in the binary Pb-Se system measured in Ref 11 and the calculated mixing enthalpies from the accepted theoretical evaluation of binary Pb-Se.^[22] The values for $x(\text{Se}) > 0.35$ published in Ref 11 are only extrapolated. This is shown in Fig. 16. An analogical problem exists for $x(\text{Se}) > 0.5$ also in the Se-Sn binary system, a comparison between the experimental measurements for the Se-Sn system from Ref 11 and accepted theoretical assessment from Ref 21 is shown in Fig. 17.

The experimental results for $x(\text{Pb})/x(\text{Se}) = 1/1$ and $2/3$ ratios are shown in Fig. 13 and 14. The agreement between the experiments and calculations for the first Pb/Se ratio is again reasonable, considering relatively high content of selenium for small Sn contents, where the discrepancy is more pronounced. On the other hand, the experimental and theoretical boundary between the liquid and the (Liq + PbSe) two-phase field is very close. An example of a significant discrepancy between experiment and modelling is demonstrated in Fig. 14. Here the samples have a relatively high selenium content, especially in the region with a low tin content. Nevertheless, there is big difference between the experiment and the calculation in the whole region and

the experimental data are problematic even in the Sn rich region. The values of the enthalpy of mixing do not go to 0 for pure tin. Since all previously presented results in Fig. 7, 8, 9, 10, 11, 12 and 13 show good or at least reasonable agreement between the experiment and the calculation, it can be assumed that the experimental values for the $x(\text{Se})/x(\text{Pb}) = 3/2$ ratio are influenced by some systematic error. Since a less reasonable agreement between calculation and experiment in all presented figures was usually obtained for samples with high selenium content, the reason for this disagreement may be the effect of the evaporation of Se in the Se-rich samples above the boiling point of pure selenium at 685°C.

The partial liquidus surface of the Pb-Se-Sn system was studied by Zlomanov et al.^[9] and the liquidus surface in the whole concentration range was presented by Saveliev et al.^[10] Unfortunately, both papers are very brief and no detailed information is provided about the samples, the experimental method, and the evaluation of results. Saveliev et al.^[10] presented only one figure in their paper, where the liquidus surface is shown. On the other hand, their results look reasonable and presented features are broadly consistent with the calculated liquidus surface. Experimental results^[10] suggest the existence of two liquid miscibility gaps, which agrees well with the calculations. The complex structure of the calculated liquidus surface with multiple strangely shaped miscibility gaps was mentioned in the discussion of Fig. 4 and 5. This structure appeared when a better agreement was sought for the position of Liquid(ter) phase field at low temperatures and high Sn solubility in the PbSe phase around 800°C and such character of the liquidus surface is not acceptable.

A comparison of the experimental and calculated liquidus surface is shown in Fig. 15(a) and (c), the detail of the region around Liquid(ter) is presented in Fig. 15(b). It can be stated that despite the experimental uncertainties, all key features are in good qualitative agreement in both figures. Theoretical calculations suggest the existence of a miscibility gap in the Se—rich corner up to high temperatures, but the equilibria at high temperatures are metastable at ambient pressure as there will be selenium gas in equilibrium with liquid and no information is available for this region.

The invariant reactions containing the liquid phase are listed in Table 3. The two ternary invariant reactions designated as D1 and D2 are degenerate reactions in nature. They lie extremely close to the binary low-temperature invariant reactions in the Pb-Sn and Se-Sn systems and the Pandat software has not been able to describe the nature of these reactions. It only lists the phases involved, not the type of reaction. After careful analysis of many calculations of isothermal sections and isopleths, the ones listed in Table 3 were identified as the most likely, but the

designation of the reactions as degenerate was retained because there is no clear evidence to support the analysis.

5 Conclusion

The literature related to the Pb-Se-Sn phase diagram is relatively sparse and there are considerable inconsistencies between the various authors. Many phase equilibria have not been well defined. The current study presents the theoretical assessment which is based on the little experimental information considered to be reliable enough to contribute to the thermodynamic modelling of Pb-Se-Sn phase diagram in whole concentration and temperature range. This assessment is part of an effort to develop a thermodynamic database for quinary Ag-Pb-Se-Sn-Te system, which is important for the further development of materials for thermoelectric applications.

The calculated phase diagram agrees reasonably with the experimental sections at 350 and 500 °C from Ref 3 especially in the region with low selenium content and a reasonable agreement was obtained with sparse information about experimental liquidus surface. Similarly, the calculated enthalpies of mixing in liquid reasonably agree with the experimental data for lower selenium content.

Despite of this, a new experimental program for the Pb-Se-Sn system focused on significant inconsistencies between older experimental works is necessary to improve the thermodynamic assessment.

Acknowledgments The authors acknowledge the financial support of the Ministry of Science and Technology of Taiwan (MOST 107-2923-E-007-005-MY3) and the Czech Science Foundation (Project 18-25660J).

References

1. C. Chang, Q. Tan, Y. Pei, Y. Xiao, X. Zhang, Y.X. Chen, L. Zheng, S. Gong, J.F. Li, J. He, and L.D. Zhao, Raising Thermoelectric Performance of n-Type SnSe via Br Doping and Pb Alloying, *RSC Adv.*, 2016, **6**, p 98216.
2. A. Zevalkink, D.M. Sniadak, J.L. Blackburn, A.J. Ferguson, M.L. Chabinyk, O. Delaire, J. Wang, K. Kovnir, J. Martin, L.T. Schelhas, T.D. Sparks, S.D. Kang, M.T. Dylla, G.J. Snyder, B.R. Ortiz, and E.S. Toberer, A Practical Field Guide to Thermoelectrics: Fundamentals, Synthesis, and Characterization, *Appl. Phys. Rev.*, 2018, **5**, p 021303.
3. S.-W. Chen, T.-Y. Huang, Y.-H. Hsu, and A. Kroupa, Phase Diagram of the Pb-Se-Sn System, *J. Electron. Mater.*, 2020, **49**(8), p 4714-4729.
4. O. Zobac, K. Buchlovska, J. Pavlu, and A. Kroupa, Thermodynamic Description of Binary System Nickel-Selenium, *J. Phase Eq. Diffus.*, 2021, **42**, p 468-478.
5. O. Zobac, K.W. Richter, and A. Kroupa, Experimental Phase Diagram of the Ag-Se-Sn System at 250, 400 and 550 °C, *J. Phase Eq. Diffus.*, 2022. <https://doi.org/10.1007/s11669-022-00943-y>

6. J.C. Wolley, and O. Berollo, Phase Studies of the Pb(1-x)Sn(x)Se, *Mat. Res. Bull.*, 1968, **3**, p 445-450.
7. A.J. Strauss, Metallurgical and Electronic Properties of Pb(1-x)Sn(x)Te, Pb(1-x)Sn(x)Se and Other IV-VI alloys, *Trans. Met. Soc. AIMIE*, 1968, **242**, p 354.
8. S. Dal Corso, B. Liautard, and J.C. Tedenac, The Pb-Sn-Se System: Phase Equilibria and Reactions in the PbSe-SnSe-Subternary, *J. Phase Equil.*, 1995, **16**(4), p 308-313.
9. V.P. Zlomanov, V.I. Shtanov, A.K. Gapeev, A.V. Novoselova, Study of the part T-X-Y projection of the Pb-Se-Sn system (in Russian). *Doklady Akademii nauk SSSR*, 346-349 (1974)
10. V.P. Saveliev, E.M. Latypov, and V.P. Zlomanov, Study of T-X-Y liquidus surface in the diagram of the Pb-Sn-Se system (in Russian), *Zh. Neorg. Khimii*, 1975, **20**, p 2006-2008.
11. K.P. Kotchi, R. Castanet, and J.-C. Mathieu, Etude Thermodynamique des Alliages Pb-Se, Sn-Se et Pb-Se-Sn, *Z. Metallkde*, 1988, **79**(2), p 102-108.
12. A. Laugier, J. Cadoz, M. Faure, and M. Moulin, Ternary Phase Diagram and Liquid Phase Epitaxy of Pb-Sn-Se and Pb-Sn-Te, *J. Cryst. Growth*, 1974, **21**, p 235-242.
13. H. Okamoto, Se-Sn (Selenium-Tin), *J. Phase Eq. Diffus.*, 1998, **19**, p 293.
14. N. Saunders, and A.P. Miodownik, *Calphad (A Comprehensive Guide)*. Pergamon Press, Oxford, 1998.
15. H.L. Lukas, S.G. Fries, and B. Sundman, *Computational Thermodynamics: The Calphad Method*. Cambridge University Press, New York, 2007.
16. J.-O. Andersson, T. Helander, L. Höglund, P. Shi, and B. Sundman, Thermo-Calc & DICTRA, Computational Tools for Materials Science, *Calphad*, 2002, **26**, p 273-312.
17. W. Cao, S.L. Chen, F. Zhang, K. Wu, Y. Yang, Y.A. Chang, R. Schmid-Fetzer, and W.A. Oates, PANDAT Software with PanEngine, PanOptimizer and PanPrecipitation for Multicomponent Phase Diagram Calculation and Materials Property Simulation, *Calphad*, 2009, **33**, p 328.
18. SGTE Unary Database, ver. 5.0, www.sgte.net/en/free-pure-substance-database
19. O. Redlich, and A. Kister, Thermodynamics of nonelectrolyte solutions—X-Y-T relations in a binary system, *Ind. Eng. Chem.*, 1948, **40**, p 341-345.
20. Y.M. Muggianu, M. Gambino, and J.P. Bros, Enthalpies of formation of liquid alloys Bismuth-Gallium-Tin at 723 K – choice of analytical representation of integral and partial thermodynamic functions of mixing for this ternary system, *J. Chim. Phys.*, 1975, **72**, p 83-88.
21. Y. Feutelais, M. Majid, B. Legendre, and S.G. Fries, Phase Diagram Investigation and Proposition of a Thermodynamic Evaluation of the Tin-Selenium System, *J. Phase Equil*, 1996, **17**, p 40-49.
22. Y. Liu, Z. Kang, G. Sheng, L. Zhang, J. Wang, and Z. Long, Phase Equilibria and Thermodynamic Basis for the Cd-Se and Pb-Se Binary Systems, *J. Electron. Mater.*, 2012, **41**(7), p 1915-1923.
23. H. Ohtani, K. Okuda, and K. Ishida, Thermodynamic Study of Phase Equilibria in the Pb-Sn-Sb System, *J. Phase Equil*, 1995, **16**(5), p 416-429.

Publisher's Note Springer Nature remains neutral with regard to jurisdictional claims in published maps and institutional affiliations.